Cellular Oncology 31 (2009) 191–201
DOI 10.3233/CLO-2009-0465
IOS Press

BRCA2 heterozygosity delays cytokinesis in primary human fibroblasts

Asta Björk Jonsdottir [a,b,c], Maaike P.G. Vreeswijk [d], Ron Wolterbeek [f], Peter Devilee [d,e], Hans J. Tanke [c], Jorunn E. Eyfjörd [a,b,*] and Karoly Szuhai [c]

[a] *Faculty of Medicine, University of Iceland, Reykjavik, Iceland*
[b] *The University of Iceland and Icelandic Cancer Society Molecular and Cell Biology Research Laboratory, University of Iceland, Reykjavik, Iceland*
[c] *Department of Molecular Cell Biology, Leiden University Medical Center, Leiden, The Netherlands*
[d] *Department of Human Genetics, Leiden University Medical Center, Leiden, The Netherlands*
[e] *Department of Pathology, Leiden University Medical Center, Leiden, The Netherlands*
[f] *Department of Medical Statistics, Leiden University Medical Center, Leiden, The Netherlands*

Abstract. *Background*: Inherited mutations in the tumour suppressor gene *BRCA2* greatly increase the risk of developing breast, ovarian and other types of cancers. So far, most studies have focused on the role of BRCA-pathways in the maintenance of genomic stability.

In this study we investigated the potential role of the BRCA2 protein in cytokinesis in unmodified primary human fibroblast carrying a heterozygous mutation in the *BRCA2* gene.

Methods: Cell divisions were monitored with time lapse live-cell imaging. *BRCA2* mRNA expression levels in $BRCA2^{+/-}$ and $BRCA2^{+/+}$ cells were quantified with quantitative real-time polymerase chain reaction (qRT-PCR). To investigate the localization of the BRCA2 protein during cytokinesis, immunofluorescence staining using antibody directed against BRCA2 was carried out. Immunofluorescence staining was performed directly after live-cell imaging and cells with delayed cytokinesis, of which the co-ordinates were saved, were automatically repositioned and visualized.

Results: We demonstrate that unmodified primary human fibroblasts derived from heterozygous *BRCA2* mutation carriers show significantly prolonged cytokinesis.

A Subset of the $BRCA2^{+/-}$ cells had delayed cytokinesis (40 min or longer) making the mean cell division time 6 min longer compared with $BRCA2^{+/+}$ cells, 33 min versus 27 min, respectively. Lower *BRCA2* mRNA expression levels were observed in the *BRCA2* heterozygous samples compared with the *BRCA2* wild type samples.

The BRCA2 protein localizes and accumulates to the midbody during cytokinesis, and no difference was detected in distribution and localization of the protein between $BRCA2^{+/-}$ and $BRCA2^{+/+}$ samples or cells with delayed cytokinesis and normal division time.

Conclusions: The delayed cytokinesis phenotype of the *BRCA2* heterozygous cells and localization of the BRCA2 protein to the midbody confirms that BRCA2 plays a role in cytokinesis. Our observations indicate that in a subset of cells the presence of only one wild type *BRCA2* allele is insufficient for efficient cytokinesis.

Keywords: BRCA2, cytokinesis, live-cell imaging, primary human fibroblasts, heterozygous phenotype

1. Introduction

Inherited mutations in the breast cancer susceptibility genes *BRCA1* and *BRCA2* greatly increase the risk of developing breast cancer, and other cancers such as ovarian and prostate cancers [14,23,31]. About 15% of breast cancer cases cluster in families and among these cases, germline mutations in *BRCA1* and *BRCA2* have been shown to account for 15–40% [25,29].

Several functions have been ascribed for the BRCA proteins, but most studies reported so far have focused on the role of BRCA-pathways in the maintenance of genomic stability. A well studied function of the

*Corresponding author: Jorunn Erla Eyfjörd, Faculty of Medicine, University of Iceland, The University of Iceland and Icelandic Cancer Society Molecular and Cell Biology Research Laboratory, Vatnsmyrarvegi 16, 101 Reykjavik, Iceland. Tel.: +354 5255825; Fax: +354 5254884; E-mail: jorunne@hi.is.

BRCA2 protein is its role in homologous recombination, where RAD51, a DNA recombinase, interacts with the BRC repeats and the C-terminus of BRCA2. BRCA2 directs RAD51 to the sites of DNA double strand breaks and this interaction has been shown to be essential for error-free homologous recombination repair [3,4]. Reduced amount of functional BRCA2 protein in heterozygous *BRCA2* mutation carriers causes insufficient repair of DNA double strand breaks, a condition that could contribute to the impairment of genomic stability. *BRCA2* heterozygosity has shown to increase sensitivity to specific DNA damaging agents, reduce RAD51 focus formation after irradiation, increase cell death and reduce growth rate [1,30].

Complete BRCA2 inactivation in tumours gives rise to chromosomal aberrations including both numerical and structural alterations, such as translocations, chromatid breaks and tri- and quadri-radial chromosomes [7,17,32].

Defects in cytokinesis can lead to mis-segregation of chromosomes and aneuploidy, which are indeed also observed in BRCA2 deficient cells [19,26].

Several studies have linked BRCA2 with progression through mitosis. BRCA2 has been found to co-localize to the centrosome in S-phase and early M-phase cells and to have a centrosomal localization signal at the C-terminus, which indicates that it might be involved in regulation of migration and duplication of the centrosome during the cell cycle [8,15,26]. The activity of the polo-like protein kinase 1 (Plk-1) is required for cytokinesis and proper metaphase/anaphase transition. Hyperphosphorylation of BRCA2, by Plk-1, in M phase and dephosphorylation of the protein when cells exit M phase implicates a potential role of BRCA2 in modulation M phase progression [6,11,18].

A new function for BRCA2 has been discovered. By examining murine embryonic fibroblasts (MEFs) it was shown that BRCA2 deficiency delays and prevents cytokinesis. *BRCA2* heterozygous ($BRCA2^{Tr/+}$) and homozygous ($BRCA2^{Tr/Tr}$) MEFs showed longer cytokinesis than wild type cells ($BRCA2^{+/+}$) when studied *ex vivo*. HeLa cells treated with BRCA2 siRNA showed almost twice as long cell division time as HeLa cells treated with control siRNA [2]. However, it is still unknown how exactly BRCA2 participates in cytokinesis and, importantly, the role of BRCA2 in cytokinesis as observed in murine fibroblasts has never been studied in human fibroblasts.

The aim of this study was to investigate if BRCA2 plays a role in cytokinesis in human fibroblasts and to study the involvement of BRCA2 in these cells in the late stages of cell division. Unmodified primary human fibroblasts, from individuals that carry the Icelandic *999del5 BRCA2* founder mutation, the Dutch *1537del4 BRCA2* mutation, and individuals that do not carry a *BRCA2* mutation, were studied [16,24]. Both *BRCA2* mutations cause premature stop codons downstream of the mutation site. In an earlier study no protein could be detected from the mutant *BRCA2 999del5* allele [13]. Cell divisions were monitored and cell division time estimated from recordings obtained with time lapse live-cell imaging. *BRCA2* mRNA expression levels were quantified with qRT-PCR and localization of the BRCA2 protein during cytokinesis was investigated.

2. Materials and methods

2.1. Unmodified primary human fibroblasts

Primary human fibroblasts derived from *BRCA2* mutation carriers and *BRCA2* wild type individuals were cultured from skin biopsies. Samples were collected in Iceland and The Netherlands. All samples were handled in a coded fashion, according to National ethical guidelines "Code for Proper Secondary Use of Human Tissue", Dutch Federation of Medical Scientific Societies. Permissions from the National Bioethics Committee in Iceland and the Icelandic Data Protection Authority were obtained for the study.

Fibroblasts were cultured in Dulbecco's Modified Eagle's Medium (DMEM), supplemented with 10% fetal bovine serum, penicillin (100 U/ml), streptomycin (0.1 mg/ml) and 2 mM L-glutamine (Invitrogen Corporation, Breda, The Netherlands). Cells were maintained at 37°C and 5% CO_2 and all experiments were carried out with cells in passage 8–15.

2.2. Study setup

A pilot study was set up by using 3 coded unmodified primary human fibroblast samples from Iceland, which were either derived from individuals carrying the Icelandic *999del5* founder mutation in the *BRCA2* gene or derived from *BRCA2* wild type individuals (FIS 1, FIS 2 and FIS 3) (Table 1). Cells were analyzed by live-cell imaging and their cell division time estimated. FIS 1 and FIS 3 had longer cell division time than FIS 2. It was confirmed that FIS 1 and FIS 3 carry the *BRCA2 999del5* deletion and FIS 2 has $BRCA2^{+/+}$ genotype. The study was continued using

Table 1
Unmodified primary human fibroblast cells

Sample	Genotype	Mutation	Origin
FIS 1	BRCA2$^{+/-}$	999del5*	Iceland
FIS 2	BRCA2$^{+/+}$	Wild type	Iceland
FIS 3	BRCA2$^{+/-}$	999del5*	Iceland
FNE 1	BRCA2$^{+/-}$	1537del4**	The Netherlands
FNE 2	BRCA2$^{+/+}$	Wild type	The Netherlands

The Human Genetic Variation Society (HGVS) nomenclature: *c.771_775del p.Asn257Lysfsx17; **c.1309_1312del p.Lys437Ilefsx22.

FIS 1 and FIS 2 and subsequently, samples from The Netherlands were added (FNE 1 and FNE 2) (Table 1) to extend the study, and to investigate the influence of different *BRCA2* mutations. Sample FNE 1 has previously been published as family D [16]. At least two separate live-cell imaging experiments (sets) were carried out for each sample and reproducibility of the estimated cell division time was calculated with 2-way ANOVA test. At least 30 cell divisions were analyzed for each sample for every set of experiments. A non-significant difference was observed between repeated experiments ($p = 0.655$) and, therefore, data sets for each sample were pooled together.

2.3. Live-cell imaging

Unmodified primary human fibroblasts were seeded on MatTek glass bottom culture dish (MatTek, Ashland, USA) and imaged when approximately 70% confluent. Cell divisions were recorded with a Leica AS MDW microscope system (Multi-Dimensional Workstation for Live Cell Imaging), consisting of an inverted phase contrast Leica DM IRE2 microscope equipped with a climate chamber and CO_2 chamber (Leica Microsystems B.V. Rijswijk, The Netherlands). Both the temperature (T) and CO_2 concentration ([CO_2]) of the medium in the culture dish were strictly controlled at all steps of the recordings ($T = 37.0^{\circ}C \pm 0.5^{\circ}C$, [$CO_2$] $5.00\% \pm 0.05\%$), as it is known that minor changes in these parameters may induce stress type conditions thereby effecting cell cycle characteristics.

Time lapse images were collected from 20 different fields from each dish with an HCX PL FL L 40×/0.60 CORR XR (3.3–1.9 mm) objective using bright field light every 5 min for up to 24 h. The Leica AS MDW software was used to generate movies from the time lapse images collected.

In order to analyze distribution and localization of the BRCA2 protein in cells with delayed cytokinesis, cells were imaged for short time (2 hours) prior to immunofluorescence staining, enabling identification of cells with prolonged cytokinesis by using relocalization.

A well known limitation of the microscopy technique applied in our study is that prolonged illumination of cells in culture may interfere with cell cycle checkpoints, particularly when cells are fluorescently stained with vital dyes or expressing fluorescent tagged proteins [21]. The use of fluorescent tagged cell cycle related proteins, such as cyclin B1-GFP, could have provided more options but in the process examined, i.e. cytokinesis, the cells have already passed all checkpoints that control the cell cycle process and the transfection per se could influence the cell characteristics and, therefore, would not be informative. However, when using unstained cells, fluorescence excitation and formation of radicals is negligible. Furthermore, cells hardly absorb light in the wavelength range between 400 and 700 nm (except erythrocytes with hemoglobin and melanocytes containing melanin), which implies that no heat is locally produced as a consequence of the absorption process using bright-field microscopy only. We, therefore, used transmitted light only to avoid any photo damage.

2.4. Quantitative real-time polymerase chain reaction (qRT-PCR)

The *BRCA2* mRNA expression levels were investigated with qRT-PCR. 0.84 μg total RNA of each sample, isolated following standard procedure using TRIzol® Reagent (Invitrogen, Breda, The Netherlands), was treated with deoxyribonuclease 1 according to the manufacturer's instructions (Sigma-Aldrich Chemie B.V., Zwijndrecht, The Netherlands). First-strand cDNA was synthesized using 50 μM oligo(dT)$_{20}$ and Super-script III transcriptase according to the manufacturer's instructions (Invitrogen, Breda, The Netherlands). Each PCR was carried out in triplicate in a 25 μl amplification mixture containing template cDNA, iQ SYBR Green Supermix (12.5 μl) (Bio-Rad Laboratories, Veenendaal, The Netherlands) and 0.4 μM BRCA2 forward and reverse primers or 0.3 μM housekeeping gene forward and reverse primers. Reactions were run on a Bio-Rad iCycler Thermal Cycler (Bio-Rad Laboratories, Hercules, CA, USA). The cycling conditions comprised 10 min polymerase activation at 95°C and 40 cycles at 95°C for 30 s and 60°C for 60 s, followed by a melting curve analysis from 58°C–95°C.

geNorm [28] was used to calculate the gene-stability for all the control genes, succinate dehydrogenase complex, subunit A (SDHA), glyceraldehyde-3-phosphate dehydreogenase (GAPDH) and hypoxanthine phosphoribosyl-transferase 1 (HPRT1). The most stably expressing control gene (SDHA) was used as a reference to calculate the normalized expression level of *BRCA2*, using the standard delta C_t method [28]. The relative values for the controls were set to one.

The sequences of the primers used for qRT-PCR were as follows: BRCA2 forward, CCAAGTGGTCCACCCCAAC, reverse, CACAATTAGGAGAAGACATCAGAAGC; SDHA forward, TGGGAACAAGAGGGCATCTG, reverse, CCACCACTGCATCAATTCATG; GAPDH forward, TTCCAGGAGCGAGATCCCT, reverse, CACCCATGACGAACATGGG and HPRT1 forward, TGACACTGGCAAAACAATGCA, reverse, GGTCCTTTTCACCAGCAAGCT.

2.5. Flow cytometry

DNA content for DNA ploidy and cell cycle analysis was measured using flow cytometry. 1.0×10^6 cells were collected and suspended in 1×Phosphate Buffered Saline (PBS). After centrifugation cells were re-suspended in 0.5 ml 1×PBS. Cell suspension was transferred into tubes containing 4.5 ml ice cold 70% ethanol. Cells were kept cold in fixative for at least 2 h. Ethanol-suspended cells were centrifuged and ethanol decanted thoroughly. Pellet was suspended in 5 ml 1×PBS and waited for 1 min before centrifugation. Pellet was then suspended in 1 ml 0.02 mg/ml Propidium Iodine (PI)/0.1% Triton X-100/1×PBS staining solution containing 2 mg RNase A. Samples were kept at 37°C for 15 min and PI emission detected at Texas red wavelength using BD LSR II Flow Cytometer and the BD FACSDiva Software (BD Biosciences, Breda, The Netherlands). The ModFit LT™ flow cytometry software was used for the data analysis (Verity Software House, Topsham, ME, USA).

2.6. Annexin V detection of apoptotic cells using live-cell imaging

To investigate the fraction of apoptotic cells staining with PI and Annexin V conjugated to the Alexa Fluor® 488 fluorophore (Alexa Fluor® 488 annexin V) was carried out using the Vybrant® Apoptosis Assay Kit #2 (Invitrogen, Breda, The Netherlands). The method for utilizing Annexin V binding on adherent cells was adjusted from published methods [27]. Cells were plated and cultured in monolayer on MatTek glass bottom culture dish. 48 hours later (when approximately 70% confluent) cells were washed twice in 1×PBS. 100 µl containing culture medium, 10 µl of Alexa Fluor® 488 annexin V and 0.2 µg/ml PI were added drop vice to the dish and incubated with 5% CO_2 at RT for 10 min, followed up immediately with live-cell imaging at 37°C and 5% CO_2. Images were collected from 20 randomly selected positions from the microscope plate with an HPX PL APO 63× 1.3GLYC 37°C objective using Leica AF6000 LX live-cell imaging system (Leica Microsystems B.V. Rijswijk, The Netherlands).

2.7. Immunofluorescence

Unmodified primary human fibroblasts were cultured on glass slides or glass bottom culture dishes for 2 days. After removing culture medium cells were washed with 1×Tris Buffered Saline (TBS), fixed for 3 min in 3.7% paraformaldehyde/1×TBS at RT and washed with 1×TBS/0.1% Triton X-100. A separate BRCA2 antibody and specimen blocking step was performed by using a blocking buffer (1×TBS/0.1% Triton X-100/2% BSA) for 2 h at RT and for 30 min at RT, respectively. Incubation with polyclonal rabbit anti-BRCA2 (kindly provided by Prof. Venkitaraman, Cambridge, England) and Aurora-B (BD Biosciences, Breda, The Netherlands) was performed at 37°C for 45 min. Specimens were washed with blocking buffer before incubation with secondary antibodies at 37°C for 30 min. BRCA2 was revealed with Cy™3-conjucated affinity-purified goat anti-rabbit antibody (Brunschwig Chemie, Amsterdam, The Netherlands) and Aurora-B with Alexa 488-conjucated goat anti-mouse antibody (Invitrogen, Breda, The Netherlands). Antibody incubation was followed by three changed washing steps with 1×TBS/0.1% Triton X-100 before mounted in Vectashield with 4′,6-diamino-2-phenylindole-dihydrochloride (DAPI)/citifluor (500 ng/ml) (Brunschwig Chemie, Amsterdam, The Netherlands). Image acquisition was performed using a DM-RA epifluorescence microscope (Leica Microsystems B.V. Rijswijk, The Netherlands) equipped with a Quantix camera (Roper Scientific, Fairfield, IA, USA). Gray scale images were collected with 100× objective by using appropriate filters to visualize Alexa 488, Cy3 and DAPI. For further image processing an in house developed software (ColourProc) was used [22].

Table 2
ANOVA statistical analysis of the cell division time of BRCA2$^{+/+}$ and BRCA2$^{+/-}$ unmodified primary human fibroblasts

	BRCA2$^{+/-}$ vs. BRCA2$^{+/+}$				BRCA2$^{+/-}$ vs. BRCA2$^{+/-}$	BRCA2$^{+/+}$ vs. BRCA2$^{+/+}$
	FIS 1 vs. FIS 2	FIS 1 vs. FNE 2	FNE 1 vs. FIS 2	FNE 1 vs. FNE 2	FIS 1 vs. FNE 1	FIS 2 vs. FNE 2
p values	<0.01	<0.01	<0.01	<0.01	0.21	0.49

2.8. Interphase-fluorescent in situ hybridization (FISH)

To investigate the cell ploidy and the frequency of bi-nuclear cells interphase-FISH was performed by using nick translation labeled D15Z1 probe to detect centromere of chromosome 15 [9] and imaged as described earlier [22].

2.9. Statistical analysis

To compare cell division times, estimated from images obtained with time lapse live-cell imaging, including the outliers because of their biological origin but not measurement errors, ANOVA's with post hoc t-test were applied, using lsd (Table 2). To evaluate the reproducibility between the sets of experiments and difference between samples, a 2-way ANOVA was performed.

Paired sample test was applied on data obtained from flow cytometry analysis to compare the fraction of cells in the G_2/M phase of the cell cycle in the BRCA2$^{+/+}$ and BRCA2$^{+/-}$ samples.

BRCA2 mRNA expression levels between *BRCA2* wild type and heterozygous mutant samples were compared by calculating delta C_t values for every sample [28] and performing a t-test on the logarithm of the normalized expression values, BRCA2$^{+/+}$ versus BRCA2$^{+/-}$.

3. Results

3.1. Heterozygous mutation in the BRCA2 gene causes delay in cytokinesis in unmodified primary human fibroblasts

3.1.1. Cell division time of BRCA2 heterozygous mutant and BRCA2 wild type cells

Cell divisions in unmodified primary human fibroblasts were monitored by time lapse live-cell imaging to study the phenotype of cells that carry a mutation in the *BRCA2* gene. Bright field microscopy was used to minimize photo damage. Under strict control of temperature and CO_2 unmodified primary human fibroblasts derived from carriers of a *BRCA2* mutation (FIS 1, *BRCA2 999del5*, and FNE 1, *BRCA2 1537del4*) and non-mutation carriers (FIS 2 and FNE 2) were analyzed (Table 1).

The cytokinesis duration, the time from metaphase (when the chromosomes are visible and are aligned in an equatorial plane) until complete cell separation (when the daughter cells and their cytoplasm have separated) was estimated (Fig. 1).

In concordance with the mutation status and in line with previously published data on murine embryonic fibroblasts [2] cells carrying a mutation in the *BRCA2* gene had on average a longer cell division time than *BRCA2* wild type cells. The mean cell division time for the BRCA2$^{+/-}$ cells FIS1 and FNE1 was 32 and 33 min, respectively, which was significant longer than for the BRCA2$^{+/+}$ cells FIS2 and FNE2 that had mean cell division time of 27 and 26 min, respectively (Fig. 2(A)). The increase in cell division time for the BRCA2$^{+/-}$ cells was observed to be highly significant when compared with the BRCA2$^{+/+}$ unmodified primary human fibroblasts (FIS 1 vs. FIS 2, $p < 0.01$; FIS 1 vs. FNE 2, $p < 0.01$; FNE 1 vs. FIS 2, $p < 0.01$ and FNE 1 vs. FNE 2, $p < 0.01$) (Table 2). There was no significant difference between the cell division time for the two *BRCA2*$^{+/+}$ samples (FIS 2 vs. FNE 2, $p = 0.49$) nor for the two BRCA2$^{+/-}$ samples (FIS 1 vs. FNE 1, $p = 0.21$) (Table 2) manifesting that the different heterozygous mutants show the same phenotype.

After pooling the cell division time for the two *BRCA2* wild type and the two *BRCA2* heterozygous mutant samples a significant increase of 6 min in the mean cell division time was observed for the BRCA2$^{+/-}$ cells, 33 min compared to 27 min for the BRCA2$^{+/+}$ cells ($p < 0.01$) (Fig. 3).

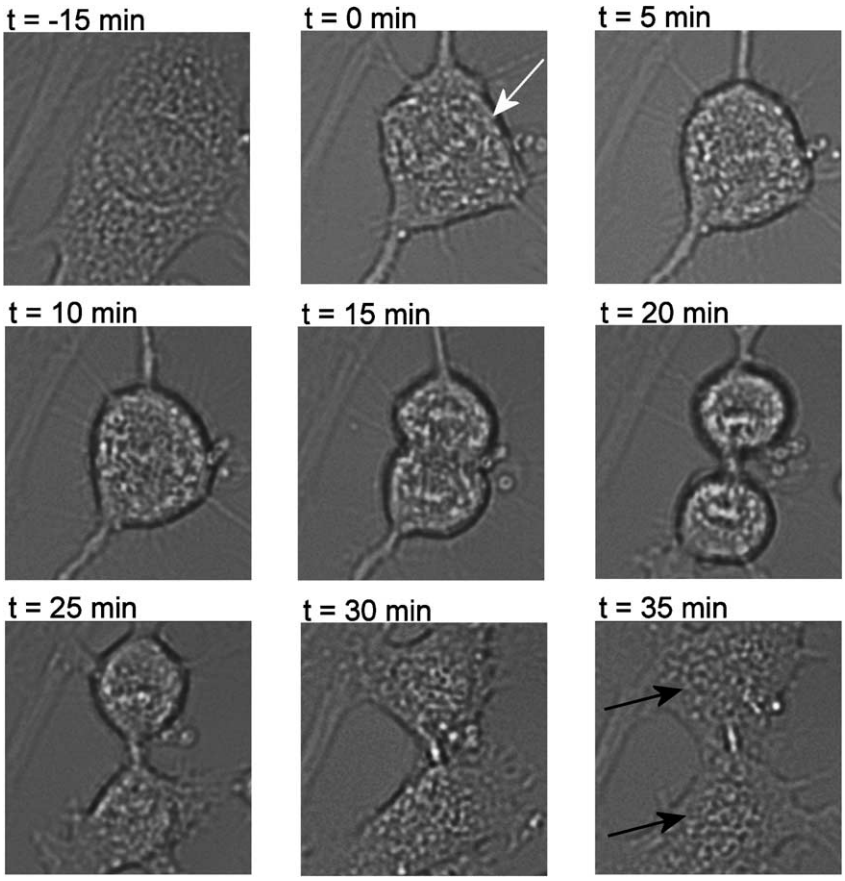

Fig. 1. Cytokinesis of unmodified primary human fibroblast. Representative time lapse images showing cell division of a BRCA2$^{+/-}$ unmodified primary human fibroblast. The cell division starts when chromosomes become visible and line up in an equatorial plane of the dividing cell ($t = 0$ min indicated by white arrow) and continues until the cytoplasm of the daughter cells has separated (black arrows indicate the end point). Cytokinesis is in this case completed in 35 min. Images were captured by time lapse live-cell imaging with a 40× objective and bright field light every 5 min.

Heterogeneity in cell division time was detected both in the *BRCA2* wild type and in the *BRCA2* heterozygous mutant samples. About 55% of the *BRCA2* wild type cells completed cell division within 25 min, for 40% the process took about 30–35 min and less than 5% had a delayed cytokinesis of 40–45 min. Of the *BRCA2* heterozygous mutant cells only 20% finished division within 25 min but for the majority (50–60%) cytokinesis took 30–35 min. Interestingly, about 20% of the *BRCA2* heterozygous cells took 40 min or longer to complete cell division, with maximum division time of 65 min (Fig. 2(A), FIS 1 and FNE 1). No cell failed to divide.

Furthermore, comparison on estimated replication time (from end of division of progenitor cell until the beginning of division of its daughter cell) in cells with delayed and normal cell division time revealed that the median replication time was approximately 20 h both for *BRCA2* wild type and heterozygous mutant samples.

3.1.2. BRCA2 mRNA expression levels

To investigate if the delay in cytokinesis in the *BRCA2* heterozygous mutant cells corresponded to lower *BRCA2* expression, a quantitative real-time polymerase chain reaction (qRT-PCR) was performed. The *BRCA2* mRNA expression levels of the two BRCA2$^{+/-}$ samples FIS 1 and FNE 1 were 0.167 and 0.254, respectively, compared with 0.987 and 1.00 for the BRCA2$^{+/+}$ samples, FIS 2 and FNE 2, respectively (Fig. 2(B)). The 5 times difference in *BRCA2* expression levels between the *BRCA2* heterozygous mutant samples and the *BRCA2* wild type samples was shown to be significant ($p = 0.03$) (Fig. 2(B)).

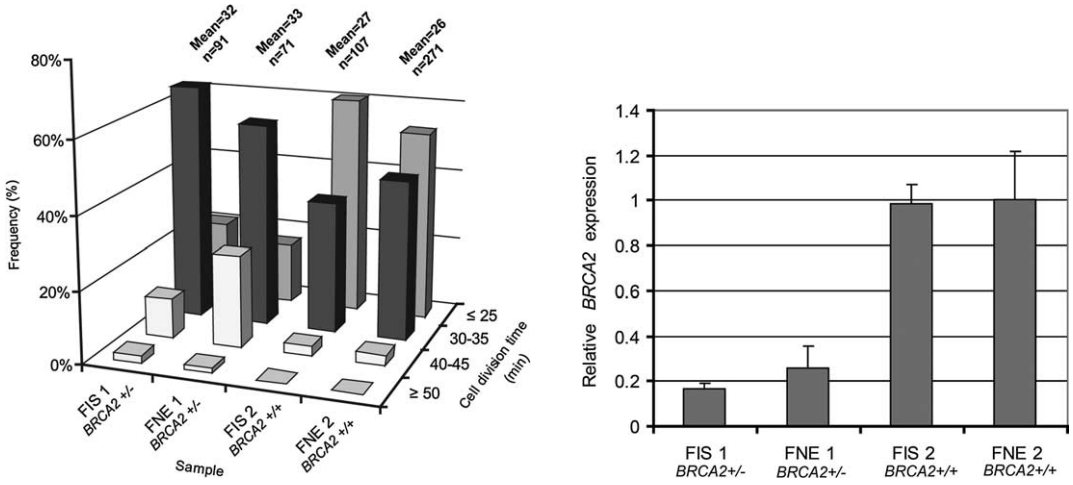

Fig. 2. Frequency distribution of the cell division time and *BRCA2* mRNA expression levlels of BRCA2$^{+/-}$ and BRCA2$^{+/+}$ unmodified primary human fibroblasts. (A) Cell division time was estimated from images obtained by time lapse live-cell imaging as shown in Fig. 1. The two BRCA2$^{+/-}$ samples, FIS 1 and FNE 1, show the same phenotype, delayed cytokinesis, but different from the two BRCA2$^{+/+}$ samples, FIS 2 and FNE 2. 50–60% of the BRCA2$^{+/+}$ cells completed cell division within 25 min and for 35–45% the process took about 30–35 min and less than 5% had a delayed cytokinesis of 40–45 min. Up to 20% of the *BRCA2* heterozygous mutant cells finished the process within 25 min but for the majority cytokinesis took 30–35 min. For about 20% of the BRCA2$^{+/-}$ cells cytokinesis proceeded for 40 min or longer with maximum cell division time of 65 min. No cell failed to divide. (B) *BRCA2* mRNA expression levels were quantified with qRT-PCR. The two BRCA2$^{+/-}$ samples, FIS 1 and FNE 1, show on average 5 times lower *BRCA2* expression than the two BRCA2$^{+/+}$ samples, FIS 2 and FNE 2, 0.167 and 0.254 versus 0.987 and 1.00, respectively. The difference between the BRCA2$^{+/-}$ and the BRCA2$^{+/+}$ samples was shown to be significant ($p = 0.03$).

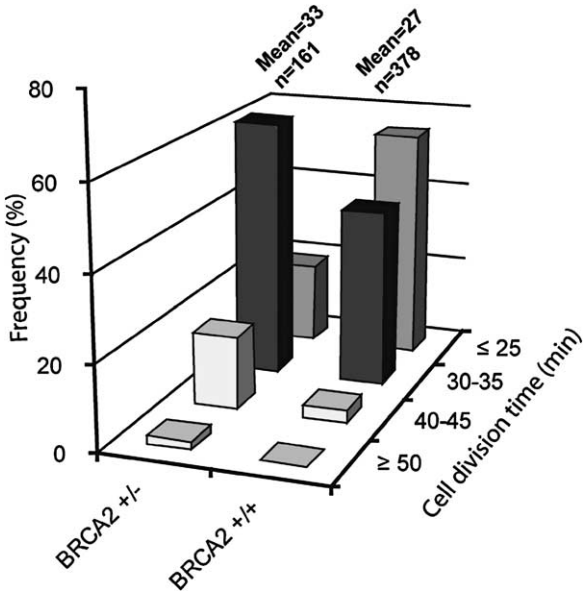

Fig. 3. Frequency distribution of the cell division time of BRCA2$^{+/-}$ versus BRCA2$^{+/+}$ unmodified primary human fibroblasts. The *BRCA2* heterozygous mutant cells have a significant longer cell division time than the *BRCA2* wild type cells, 6 min on average, indicating that the delay is associated with the mutation status in the *BRCA2* gene.

3.1.3. Fluorescent in situ hybridization (FISH) to investigate endo-reduplication

To investigate if the delayed cell division time was due to endo-reduplication, the frequency of binuclear cells and the cell ploidy was examined with interphase-FISH using probe against the centromere of chromosome 15. Four signals were detected in 6 of 478 (1.26%) and three signals in 2 of 478 analyzed BRCA2$^{+/-}$ cells (0.4%). This frequency was similar to normal cells (data not shown).

3.1.4. Flow cytometry and Alexa Fluor® 488 annexin V staining for ploidy and apoptosis estimation

Since mitotic defects can lead to increase in aneuploidy [20], we performed DNA flow cytometry. Aneuploid cell populations were not found. The BRCA2$^{+/-}$ cells did, however, have an increased fraction of cells in G_2/M phase of the cell cycle (2.22%) or 3.8× higher than in the BRCA2$^{+/+}$ samples. Statistical analysis showed the difference to be non-significant ($p = 0.49$).

To take into account the possibility that aneuploid cells undergo apoptosis the fraction of early apoptotic cells was measured by staining cells with Alexa Fluor® 488 annexin V and propidium iodide (PI) followed up

by live-cell imaging. No increase in cell death was observed in the *BRCA2* heterozygous cells compared with *BRCA2* wild type cells.

3.2. *BRCA2 localizes to the midbody of unmodified primary human fibroblasts in cytokinesis*

3.2.1. *Localization of BRCA2 in BRCA2$^{+/-}$ and BRCA2$^{+/+}$ cells during cytokinesis*

Numerous proteins, like Aurora B kinase in a complex with inner centromere protein, survivin and CSC-1, have been demonstrated to concentrate on the central spindle during cytokinesis [5]. To investigate the role of the BRCA2 protein during cytokinesis, its distribution and localization was examined in cells in cytokinesis by performing a double-immunofluorescence staining with antibodies directed against BRCA2 and Aurora B. The staining was both carried out in *BRCA2* wild type and *BRCA2* heterozygous mutant unmodified primary human fibroblasts.

The immunofluorescence staining revealed that BRCA2 localizes to the midbody in cells in cytokinesis (Fig. 4) as previously described [2]. Accumulation of the protein to the midbody increased as the process proceeded (Fig. 4) and concentrated adjacent to Aurora B in the abscission phase (Fig. 4, inset). A similar variation of the distribution of the BRCA2 protein along the midbody was observed both in BRCA2$^{+/+}$ and BRCA2$^{+/-}$ cells.

3.2.2. *Localization of BRCA2 in cells with delayed cytokinesis*

To investigate the localization of the BRCA2 protein in the sub-populations of cells with division time of 40 min or longer (delayed cytokinesis) observed in the BRCA2$^{+/-}$ samples (FIS 1 and FNE 1) (Fig. 2(A)), cell division was monitored with live-cell imaging for short time (2 hours) and followed up with immunofluorescence detection with BRCA2 and Aurora B antibodies. A computerized scanning stage and mapping of the x/y coordinates was used to relocate the cells of interest after the staining. In this way the BRCA2 staining pattern could be linked to particular cells allowing investigation of the BRCA2 protein distribution in cells with delayed cytokinesis specifically and compare it to cells with normal division time. These experiments showed no detectable difference of BRCA2 distribution between cells with normal or delayed cytokinesis.

4. Discussion

The role of the BRCA2 protein during cytokinesis was investigated in heterozygous *BRCA2* mutated human fibroblasts using live-cell imaging. This is an accurate and efficient technique to study individual cells, the cell cycle process in addition to the location, movement and interaction of cells and cell particles, cell behavior and phenotype *ex-vivo*.

Cell division time of unmodified primary human fibroblasts was estimated from images collected with time lapse live-cell imaging. Samples were obtained from individuals that carry different *BRCA2* mutations (Table 1). By comparing the cell division times of BRCA2$^{+/-}$ deletion mutants with BRCA2$^{+/+}$ cells, we observed, in concordance with the mutation status, that the BRCA2$^{+/-}$ cells had a significant delay. The mean cell division time of the BRCA2$^{+/-}$cells was shown to be 6 min longer than for the BRCA2$^{+/+}$ cells that completed the process in 27 min on average (Fig. 3). The cell division time was heterogeneous within samples. Cells with delayed cytokinesis (40 min

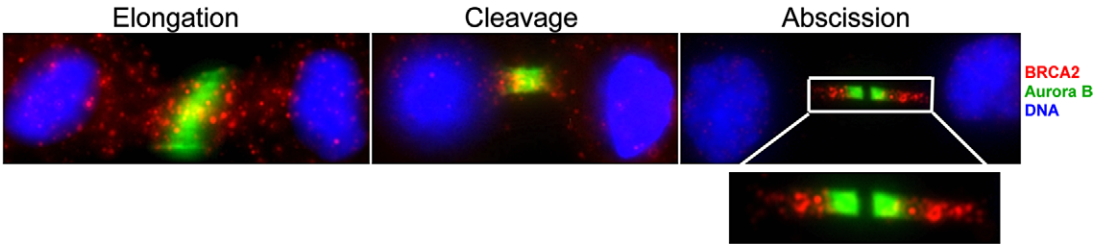

Fig. 4. Representative images of unmodified primary human fibroblasts after immunofluorescence staining to detect BRCA2 and Aurora B. Localization of the BRCA2 protein was investigated in cells in cytokinesis using polyclonal rabbit anti-BRCA2 (red) and monoclonal mouse anti-Aurora B (green) antibodies and DAPI (blue). In early steps of cytokinesis (elongation) little amount of BRCA2 is present between the forming daughter cells and mainly dispersed through out the nucleus. As the process proceeds, from elongation to cleavage phase, the accumulation of BRCA2 to the midbody increases and concentrates adjacent to the Aurora B kinase in the abscission phase as indicated by inset.

or longer) comprise a subset of the *BRCA2* heterozygous cell population, about 20%, as shown in Fig 2(A). Our data are in accordance with published data on murine cells. MEFs homozygous for a targeted *BRCA2* mutation ($BRCA2^{Tr/Tr}$) have severely extended cell division time compared with wild type and heterozygous cells. Cytokinesis was prevented in more than 30% cases in the $BRCA2^{Tr/Tr}$ murine fibroblasts and HeLa cells treated with BRCA2 siRNA [2].

The qRT-PCR results denote a correlation between lower expression levels of *BRCA2* mRNA with a delay in cytokinesis in the $BRCA2^{+/-}$ cells, where both of the $BRCA2^{+/-}$ samples studied showed similar and a relatively low expression levels The *BRCA2* wild type samples showed on average 5× higher *BRCA2* expression than the heterozygous mutant samples (Fig. 2(B)), suggesting that reduction of *BRCA2* is a rate limiting factor in this process.

The replication time of the cells did not vary between cells with different cell division time. These observations indicate that the delayed cytokinesis is not caused by replication related mechanisms [3,12].

Cytokinesis defects in *BRCA2* heterozygous cells might increase the number of aneuploid cells which then could predispose to carcinogenesis. Flow cytometry showed that $BRCA2^{+/-}$ cells accumulate in G_2/M phase of the cell cycle 3.8× more frequently than $BRCA2^{+/+}$ cells, which is in line with the 4× increase in number of cells that showed delayed cytokinesis compared with $BRCA2^{+/+}$ samples. As aneuploidy is defined as an additional G_0/G_1 peak with a small G_2/M peak and because both G_2/M diploids and G_0/G_1 tetraploids are 4N, the groups are un-distinguishable by flow cytometry [10,20].

Those results indicate that BRCA2 participates in the cytokinesis process.

The distribution and localization of BRCA2 was examined to investigate further the role of BRCA2 during cytokinesis. Immunofluorescence staining using antibodies to detect BRCA2 and the Aurora B kinase, which is known to localize and function at the midbody [5] revealed that BRCA2 localizes to the midbody in cells in cytokinesis and the accumulation increases as the process proceeds. This indicates that BRCA2 might affect or facilitate the organization of the central spindle and/or progression through cytokinesis. To investigate the molecular mechanism causing the delay in cytokinesis, observed in the $BRCA2^{+/-}$ samples, time lapse images were collected for short period (2 hours) with live-cell imaging and followed-up by immunofluorescence staining. We observed no difference in BRCA2 distribution between cells with prolonged division time ($\geqslant$40 min) and normal cell division time. Therefore, we conclude that the delayed cytokinesis phenotype is not directly linked to abnormal localization of the BRCA2 protein to the midbody.

BRCA2 is known to preserve chromosome structure and abnormal cytokinesis in *BRCA2* deficient cells may be an additional cause for chromosomal instability, a hallmark of genomic instability that contributes to tumorigenesis [7].

5. Conclusions

Our data reveal that primary human fibroblasts derived from $BRCA2^{+/-}$ individuals show significantly longer cell division time compared with $BRCA2^{+/+}$ cells, indicating that BRCA2 plays a role in cytokinesis.

Acknowledgements

We thank Prof. Helga M. Ögmundsdottir, Department of Medicine, University of Iceland, Reykjavik, Iceland and Dr. H.H. Kampinga, Cellbiology, UMC Groningen, Groningen, The Netherlands, for contributing samples, Prof. A. Venkitaraman, University of Cambridge, England, for donating BRCA2 antibody, Marja v.d. Burg for performing interphase-FISH, Jan Slats for assisting with flow cytometry analysis and Hans Baelde for qRT-PCR assistance. This work was funded by the Icelandic Center for Research Biomedicine Programme and the Margret Bjorgulfsdottir Memorial Fund. M.P.G.V. was funded by the Dutch Cancer Society (2001-2471).

References

[1] K. Arnold, M.K. Kim, K. Frerk, L. Edler, L. Savelyeva, P. Schmezer and R. Wiedemeyer, Lower level of BRCA2 protein in heterozygous mutation carriers is correlated with an increase in DNA double strand breaks and an impaired DSB repair, *Cancer Lett.* **243** (2006), 90–100.

[2] M.J. Daniels, Y. Wang, M. Lee and A.R. Venkitaraman, Abnormal cytokinesis in cells deficient in the breast cancer susceptibility protein BRCA2, *Science* **306** (2004), 876–879.

[3] A.A. Davies, J.Y. Masson, M.J. McIlwraith, A.Z. Stasiak, A. Stasiak, A.R. Venkitaraman and S.C.West, Role of BRCA2 in control of the RAD51 recombination and DNA repair protein, *Mol. Cell.* **7** (2001), 273–282.

[4] F. Esashi, V.E. Galkin, X.Yu, E.H. Egelman and S.C. West, Stabilization of RAD51 nucleoprotein filaments by the C-terminal region of BRCA2, *Nat. Struct. Mol. Biol.* **14** (2007), 468–474.

[5] M. Glotzer, The molecular requirements for cytokinesis, *Science* **307** (2005), 1735–1739.

[6] D.M. Glover, Polo kinase and progression through M phase in Drosophila: a perspective from the spindle poles, *Oncogene* **24** (2005), 230–237.

[7] S. Gretarsdottir, S. Thorlacius, R. Valgardsdottir, S. Gudlaugsdottir, S. Sigurdsson, M. Steinarsdottir, J.G. Jonasson, K. Anamthawat-Jonsson and J.E. Eyfjord, BRCA2 and p53 mutations in primary breast cancer in relation to genetic instability, *Cancer Res.* **58** (1998), 859–862.

[8] X. Han, H. Saito, Y. Miki and A. Nakanishi, A CRM1-mediated nuclear export signal governs cytoplasmic localization of BRCA2 and is essential for centrosomal localization of BRCA2, *Oncogene* **27** (2007), 2969–2977.

[9] M.J. Higgins, H.S. Wang, I. Shtromas, T. Haliotis, J.C. Roder, J.J. Holden and B.N. White, Organization of a repetitive human 1.8 kb KpnI sequence localized in the heterochromatin of chromosome 15, *Chromosoma* **93** (1985), 77–86.

[10] M. Levitus, H. Joenje and J.P. de Winter, The Fanconi anemia pathway of genomic maintenance, *Cell. Oncol.* **28** (2006), 3–29.

[11] H.R. Lin, N.S. Ting, J. Qin and W.H. Lee, M phase-specific phosphorylation of BRCA2 by Polo-like kinase 1 correlates with the dissociation of the BRCA2-P/CAF complex, *J. Biol. Chem.* **278** (2003), 35979–35987.

[12] M. Lomonosov, S. Anand, M. Sangrithi, R. Davies and A.R. Venkitaraman, Stabilization of stalled DNA replication forks by the BRCA2 breast cancer susceptibility protein, *Genes Dev.* **17** (2003), 3017–3022.

[13] E.K. Mikaelsdottir, S. Valgeirsdottir, J.E. Eyfjord and T. Rafnar, The Icelandic founder mutation BRCA2 999del5: analysis of expression, *Breast Cancer Res.* **6** (2004), R284–R290.

[14] Y. Miki, J. Swensen, D. Shattuck-Eidens, P.A. Futreal, K. Harshman, S. Tavtigian, Q. Liu, C. Cochran, L.M. Bennett and W. Ding, A strong candidate for the breast and ovarian cancer susceptibility gene BRCA1, *Science* **266** (1994), 66–71.

[15] A. Nakanishi, X. Han, H. Saito, K. Taguchi, Y. Ohta, S. Imajoh-Ohmi and Y. Miki, Interference with BRCA2, which localizes to the centrosome during S and early M phase, leads to abnormal nuclear division, *Biochem. Biophys. Res. Commun.* **355** (2007), 34–40.

[16] B. Nieuwenhuis, A.J. Assen-Bolt, M.A. Waarde-Verhagen, R.H. Sijmons, A.H. Van der Hout, T. Bauch, C. Streffer and H.H. Kampinga, BRCA1 and BRCA2 heterozygosity and repair of X-ray-induced DNA damage, *Int. J. Radiat. Biol.* **78** (2002), 285–295.

[17] K.J. Patel, V.P. Yu, H. Lee, A. Corcoran, F.C. Thistlethwaite, M.J. Evans, W.H. Colledge, L.S. Friedman, B.A. Ponder and A.R. Venkitaraman, Involvement of BRCA2 in DNA repair, *Mol. Cell.* **1** (1998), 347–357.

[18] Y.S. Seong, K. Kamijo, J.S. Lee, E. Fernandez, R. Kuriyama, T. Miki and K.S. Lee, A spindle checkpoint arrest and a cytokinesis failure by the dominant-negative polo-box domain of Plk1 in U-2 OS cells, *J. Biol. Chem.* **277** (2002), 32282–32293.

[19] Q. Shi and R.W. King, Chromosome nondisjunction yields tetraploid rather than aneuploid cells in human cell lines, *Nature* **437** (2005), 1038–1042.

[20] I.S. Smirnova, N.D. Aksenov, E.V. Kashuba, P. Payakurel, V.V. Grabovetsky, A.D. Zaberezhny, M.S. Vonsky, L. Buchinska, P. Biberfeld, J. Hinkula and M.G. Isaguliants, Hepatitis C virus core protein transforms murine fibroblasts by promoting genomic instability, *Cell. Oncol.* **28** (2006), 177–190.

[21] L. Song, C.A. Varma, J.W. Verhoeven and H.J. Tanke, Influence of the triplet excited state on the photobleaching kinetics of fluorescein in microscopy, *Biophys. J.* **70** (1996), 2959–2968.

[22] H.J. Tanke, J. Wiegant, R.P. van Gijlswijk, V. Bezrookove, H. Pattenier, R.J. Heetebrij, E.G. Talman, A.K. Raap and J. Vrolijk, New strategy for multi-colour fluorescence *in situ* hybridisation: COBRA: COmbined Binary RAtio labelling, *Eur. J. Hum. Genet.* **7** (1999), 2–11.

[23] S.V. Tavtigian, J. Simard, J. Rommens, F. Couch, D. Shattuck-Eidens, S. Neuhausen, S. Merajver, S. Thorlacius, K. Offit, D. Stoppa-Lyonnet, C. Belanger, R. Bell, S. Berry, R. Bogden, Q. Chen, T. Davis, M. Dumont, C. Frye, T. Hattier, S. Jammulapati, T. Janecki, P. Jiang, R. Kehrer, J.F. Leblanc, J.T. Mitchell, J. McArthur-Morrison, K. Nguyen, Y. Peng, C. Samson, M. Schroeder, S.C. Snyder, L. Steele, M. Stringfellow, C. Stroup, B. Swedlund, J. Swense, D. Teng, A. Thomas, T. Tran, M. Tranchant, J. Weaver-Feldhaus, A.K. Wong, H. Shizuya, J.E. Eyfjord, L. Cannon-Albright, M. Tranchant, F. Labrie, M.H. Skolnick, B. Weber, A. Kamb and D.E. Goldgar, The complete BRCA2 gene and mutations in chromosome 13q-linked kindreds, *Nat. Genet.* **12** (1996), 333–337.

[24] S. Thorlacius, G. Olafsdottir, L. Tryggvadottir, S. Neuhausen, J.G. Jonasson, S.V. Tavtigian, H. Tulinius, H.M. Ogmundsdottir and J.E. Eyfjord, A single BRCA2 mutation in male and female breast cancer families from Iceland with varied cancer phenotypes, *Nat. Genet.* **13** (1996), 117–119.

[25] H. Tulinius, G.H. Olafsdottir, H. Sigvaldason, A. Arason, R.B. Barkardottir, V. Egilsson, H.M. Ogmundsdottir, L. Tryggvadottir, S. Gudlaugsdottir and J.E. Eyfjord, The effect of a single BRCA2 mutation on cancer in Iceland, *J. Med. Genet.* **39** (2002), 457–462.

[26] A. Tutt, A. Gabriel, D. Bertwistle, F. Connor, H. Paterson, J. Peacock, G. Ross and A. Ashworth, Absence of BRCA2 causes genome instability by chromosome breakage and loss associated with centrosome amplification, *Curr. Biol.* **9** (1999), 1107–1110.

[27] M. van Engeland, F.C. Ramaekers, B. Schutte and C.P. Reutelingsperger, A novel assay to measure loss of plasma membrane asymmetry during apoptosis of adherent cells in culture, *Cytometry* **24** (1996), 131–139.

[28] J. Vandesompele, K. De Preter, F. Pattyn, B. Poppe, N. Van Roy, A. De Paepe and F. Speleman, Accurate normalization of real-time quantitative RT-PCR data by geometric averaging of multiple internal control genes, *Genome Biol.* **3** (2002), RESEARCH0034.

[29] A.R. Venkitaraman, Cancer susceptibility and the functions of BRCA1 and BRCA2, *Cell* **108** (2002), 171–182.

[30] M. Warren, C.J. Lord, J. Masabanda, D. Griffin and A. Ashworth, Phenotypic effects of heterozygosity for a BRCA2 mutation, *Hum. Mol. Genet.* **12** (2003), 2645–2656.

[31] R. Wooster, G. Bignell, J. Lancaster, S. Swift, S. Seal, J. Mangion, N. Collins, S. Gregory, C. Gumbs and G. Micklem, Identification of the breast cancer susceptibility gene BRCA2, *Nature* **378** (1995), 789–792.

[32] V.P. Yu, M. Koehler, C. Steinlein, M. Schmid, L.A. Hanakahi, A.J. van Gool, S.C. West and A.R. Venkitaraman, Gross chromosomal rearrangements and genetic exchange between nonhomologous chromosomes following BRCA2 inactivation, *Genes Dev.* **14** (2000), 1400–1406.